LBWG memo 2

Delay and phase transfer in the survey test field

Neal Jackson, 2018.05.05, updated 2018.08.14

1. The problem

The long-baseline pipeline (version 03.2018) assumes that we can use a single LBCS calibrator in the field in order to calibrate delays for the whole field, as well as making an initial phase calibration. The delay calibration is then propagated by default through the field, and the phase calibration is iterated on successively fainter sources. The assumption is that the initial phase calibration is good enough to remove the fast variation, so that subsequent phase calibration can be used to remove the slower variation.

This document attempts to answer two questions:

- If we use a single delay correction, will this be OK for the whole field? If the residual delay is big enough, the result will be decorrelation when using a wide bandwidth. **An uncorrected delay of x nanoseconds will result in decorrelation over a bandwidth of $1000/x$ MHz, so if mapping the whole bandwidth, any residual delay must be <20 ns.**
- To what extent does the solution time for phase corrections increase if a phase calibration is done on a bright source?

In order to answer these questions we use the standard test field (Memo 1) and perform initial solutions on 1327+5504. These solutions are then evaluated by looking at their effect on 1349+5431, which is approximately 4 degrees distant at the other end of the field. In many cases distances smaller than this will be typical, if the calibrator source is in the middle of the field - but in many cases, the ionosphere will be worse than that which is present in the test field observations.

2. Delay transfer

100 subbands were used, and smaller datasets were formed around each of the two positions by 4× frequency and time averaging. The delay and phase correction was done in AIPS at the 1327+5504 position by the following algorithm:

- Divide the bandwidth into 8 and make independent solutions in all cases for each of the 8 subbands.
- Solve for non-dispersive delay and phase, without rates, with 5-minute solution intervals and using all antennas, and calibrating against a previously made good model. Throw away the phase solutions (since unlike delay, the phase varies over a much shorter timescale than this).
- Edit (with a 50-ns cut over a boxcar length of 2h) and smooth the delay solutions (with a timescale of 1h), and apply them.
- Solve the phases with a 30-second solution interval. (This is only just short enough for the longest baselines).

Dynamic phase plots are shown for the calibrated data in Fig.**??**, which shows the amplitude, the phases after correction (using 8 subbands) and the phases after correction

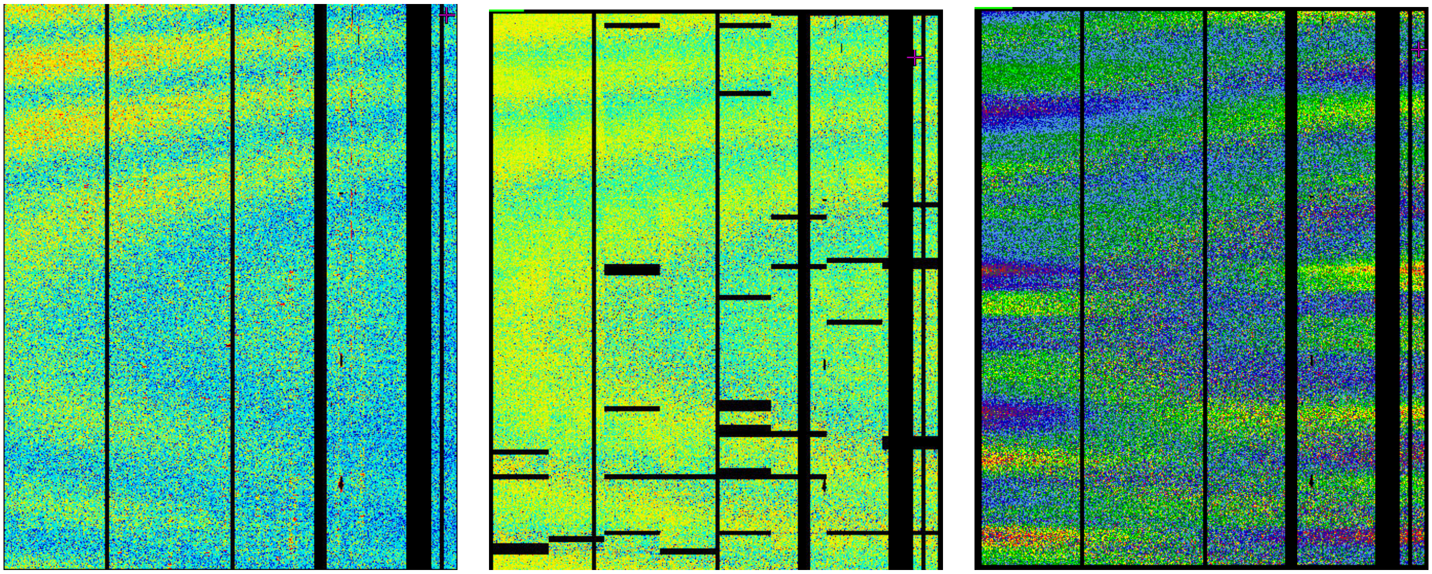

Figure 1: Amplitude (L) and phase (middle) against frequency (x) and time (y) for delay and phase corrected data on 1327+5504. The ST001-UK608 baseline has been used (as this should be close to the worst-case). Note the structure on the source which is left over after correction, and in which the phase structure resembles the amplitude structure. The correction using only one non-dispersive delay across the whole 20-MHz band (R) is disastrous, although it is obviously approximately correct across each 2.5-MHz subband.

(using all the data together). The latter procedure is obviously disastrous, the reason being that dispersive delay across the band is averaged over. Since 1327+5504 is a relatively simple double source, the phase structure, when properly corrected, should look like the amplitude structure.

We then transfer these solutions across 4° and apply them to 1349+5341. This is a resolved source without much structure, as seen by the featureless amplitude as a function of time and frequency, which nevertheless has coherent signal on all baselines. Applying an incremental phase and delay solution, derived in the same way as 1327+5504, allows a complete removal of features in both frequency and time directions (Fig. **??**).

Fig. **??** shows the incremental delays - due to the differential ionosphere over a 4° displacement - between the calibrator 1327+5504 and the source 1349+5431. Delays are pretty consistent in form between IFs, but vary in size between IFs (as would be expected from a dispersive delay). The differential delay is generally about 20 ns, although rather larger for the more distant stations. Fig **??** shows the equivalent quantity for the phases. Here, there has been a definite lengthening of the typical phase coherence time from about one minute to about 5 minutes, or up to 10 minutes in the best cases.

Conclusion of the foregoing

Delay and phase calibration at one part of a Lofar-LB field improves delay and phase variations at other parts of the field but does not eliminate them. In the LB test field, delay excursions of about 20 ns, or rather longer, remain in the data at a point 4° from the calibrator. This implies decoherence across a band of 40 MHz, although the decoherence should be negligible in bands of less than 10 MHz. It implies that multiple delay calibrators may need to be used in each field where possible. Phase coherence times, as expected,

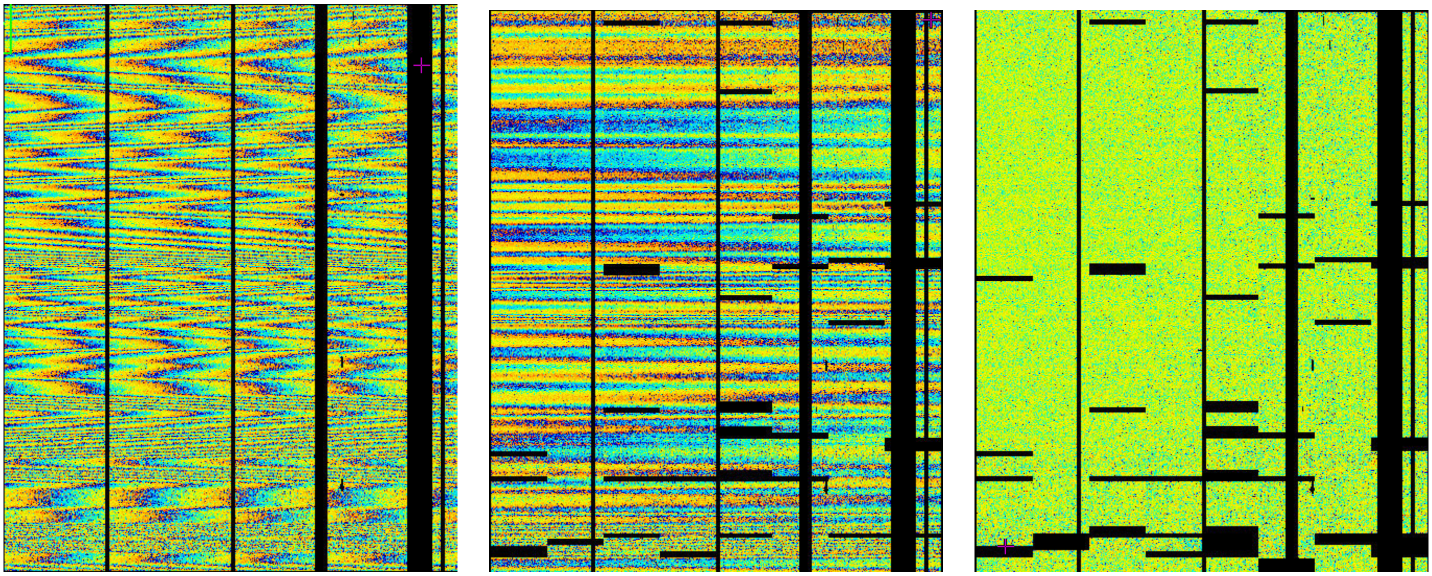

Figure 2: Left: uncalibrated dynamic phase spectrum of 1349+5431. Centre: After application of solutions from 1327+5504. Note that there is some remaining delay, amounting to a large part of a turn across the band at some times. Right: after complete removal of phases and delays.

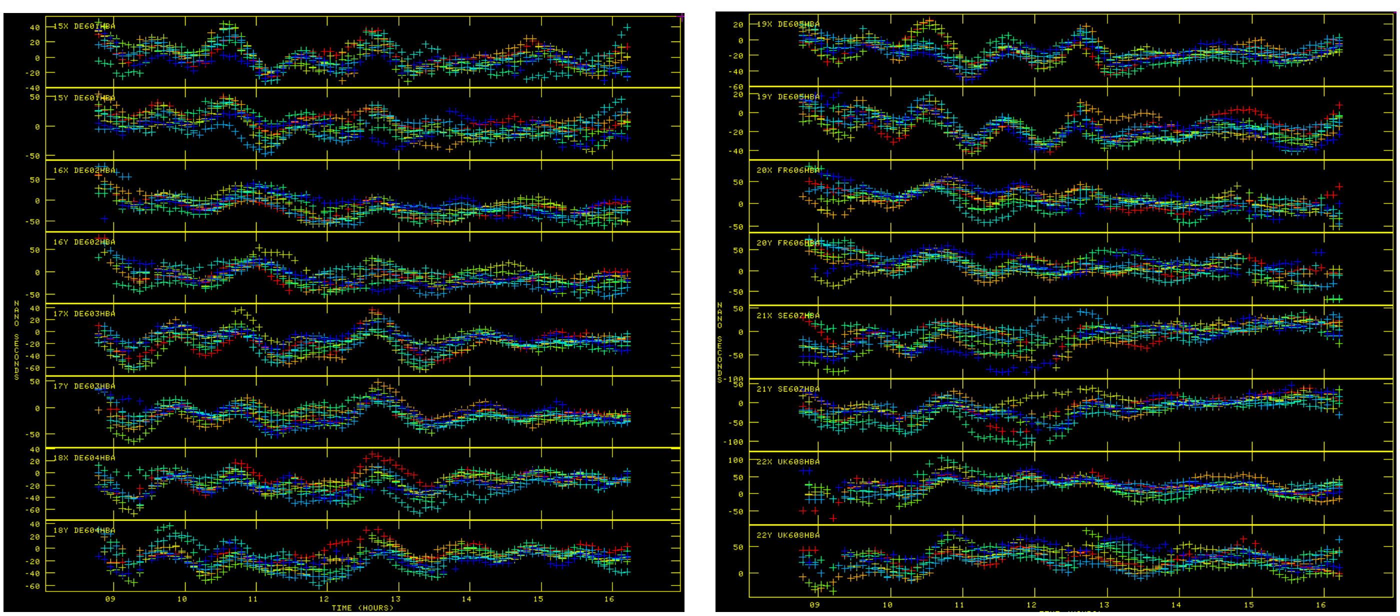

Figure 3: Incremental delay solutions on 1349+5431, *after* application of delays from the primary calibrator. Delays of up to 20 ns are seen which corresponds to decorrelation over 50 MHz bandwidths.

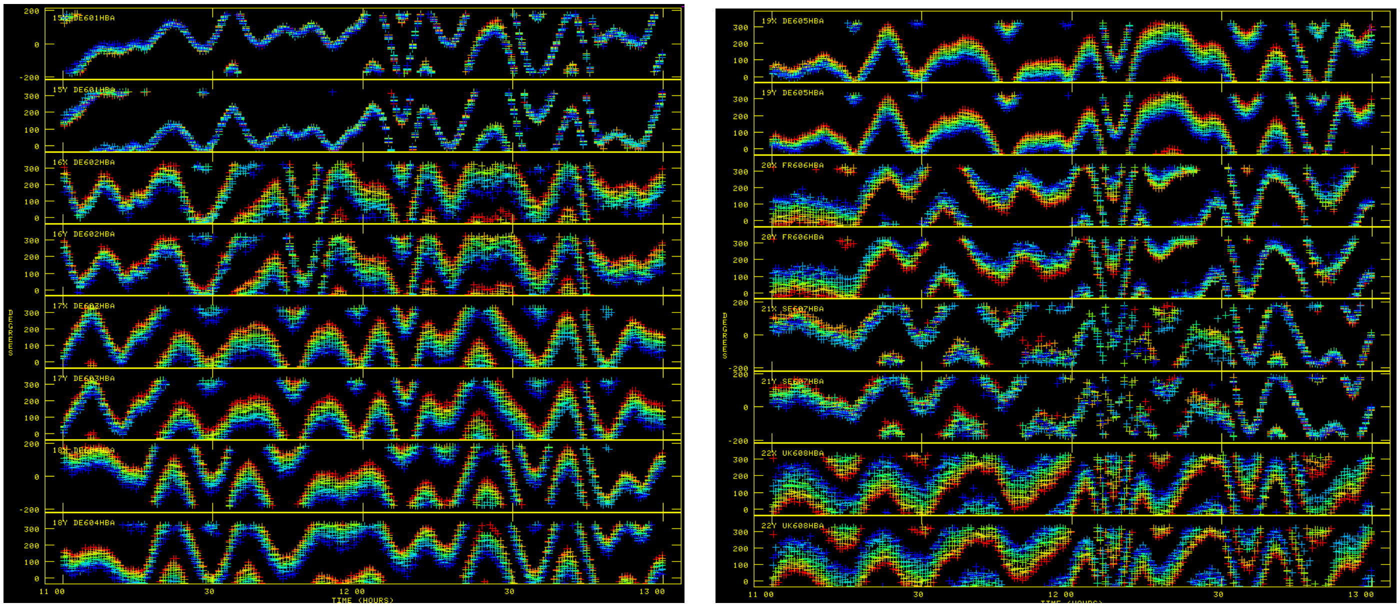

Figure 4: Incremental phase solutions on 1349+5431 on international stations (DE601-UK608), *after* application of delays from the primary calibrator. Phase variations, originally on timescales of 0.5-2 minutes, have generally been converted to longer-timescale variations of ∼5-10 minutes by application of the original correction.

increase by use of an in-field calibrator, typically by a factor of a few.

More systematic investigations with LBCS sources

(in progress)

Figure**??** shows closure statistics for all LBCS sources within 2.5 degrees of the field centre, and which are mostly or all 'P' (well detected) by LBCS. Worryingly, a few are not visible in dynamic spectra, but most can be seen and calibrated on, even if the closure statistic is quite low. **To do:** investigate those for which this is not true.

L1324+5454	15.3	3.7	7.1	7.3	61.5	1.3	1.7	3.1
L1325+5540	6.4	3.4	0.5	3.3	34.4	0.0	2.4	3.3
L1326+5514	27.3	6.4	21.5	12.9	47.5	3.5	5.7	0.4
L1326+5637	1.1	0.0	2.3	2.0	2.8	3.3	2.3	3.3
L1327+5504	147.0	58.7	148.9	130.6	280.3	49.6	62.0	41.0
L1330+5546	3.1	3.2	3.3	3.3	28.9	1.6	0.0	1.7
L1334+5631	1.6	2.1	2.3	0.8	3.0	3.5	1.3	1.5
L1335+5631	3.2	0.3	1.6	2.8	4.9	1.4	2.1	2.0
L1337+5501	10.9	13.2	17.8	15.8	27.4	15.8	14.1	12.3
L1339+5257	1.5	1.4	1.3	1.3	4.8	3.9	3.2	3.2
L1339+5638	3.6	2.1	6.5	3.7	17.2	3.2	1.0	3.0
L1341+5415	5.4	2.7	7.1	9.7	13.6	4.5	2.0	7.8
L1342+5707	1.1	2.1	2.6	2.8	1.2	4.6	2.6	2.7
L1342+5717	3.0	2.1	0.9	1.5	3.2	1.1	0.8	0.9
L1343+5253	2.4	4.0	0.9	0.1	0.9	2.8	2.2	1.4
L1344+5233	0.0	3.0	0.0	1.5	0.7	0.2	2.3	1.4
L1344+5348	2.7	3.1	3.1	1.4	2.3	0.1	2.4	2.4
L1344+5503	4.2	8.9	17.8	17.9	19.1	3.9	2.5	3.8
L1344+5658	0.5	3.4	0.0	2.4	2.1	3.2	1.8	3.0
L1347+5647	3.7	1.3	2.0	2.9	1.3	3.6	1.1	2.0
L1349+5341	34.5	14.1	28.9	32.1	78.6	25.5	21.3	20.7
L1350+5447	1.4	2.9	3.7	4.0	3.0	4.7	2.8	1.8
L1351+5306	1.7	1.0	0.9	2.4	4.5	0.0	3.9	3.2
L1351+5518	10.2	2.4	4.0	3.0	29.4	0.8	2.7	2.0
L1352+5458	3.2	3.1	3.6	2.9	2.8	2.8	3.3	1.4
L1353+5610	0.5	2.1	4.4	1.9	4.5	0.9	3.0	3.6
L1353+5725	2.3	1.0	3.4	2.7	1.2	2.5	3.0	4.7
L1354+5520	2.9	1.0	0.9	4.2	3.9	2.9	2.1	2.2
L1354+5650	9.6	1.1	1.0	1.6	2.2	5.0	3.4	2.0
L1355+5540	2.7	0.0	3.1	3.2	4.4	0.0	4.1	1.7
L1355+5614	1.4	1.7	2.1	3.0	0.9	2.0	0.0	1.9
L1356+5339	1.3	1.1	4.9	1.3	1.0	3.2	2.0	1.9
L1356+5630	4.4	2.6	3.3	1.8	2.0	1.7	2.6	1.8

Figure 5: Closure statistics for LBCS sources

The primary calibrator source 1327+5504 has been fitted for phase and delay, using a hand-generated model, and transferred to the rest of the field. Movies have been produced of the phase and delay response for each antenna across the field which are available on

`http://www.jb.man.ac.uk/~njj/movie_ionosphere.tar`

There is one file for each antenna. Quick notes at this stage:

- The colour scheme for phases is a colour circle red→blue→green→red. For delays, zero delay is white and large positive and negative delays are pink and yellow.

- 1327+5504 is the reference for everything (constant cyan in phases and white in delays).

- Large circles are the brighter (better closure statistic) sources.

- The major problem with generating these plots is that intrinsic source structure mimics time-dependent phase variation in the ionosphere. This requires making a model of each source and then re-calculating the differential phase correction against the model. This is not working perfectly yet, in particular for the bright source 1349+5341 whose colour changes quite rapidly.

- For most antennas the results are moderately encouraging; there are long periods of coherence which suggest that phase can be transferred a long way across the field for at least half the time. Even with incomplete calibrator coverage, an option could be to select just the coherent times in order to image fainter sources.

- Even the more distant stations (see e.g. SE607) have considerable coherence within a degree or two.

- The preliminary script (`plotfield.py`) is on the github site `nealjackson/lofar-lb`. It is written in parseltongue, but keeps the AIPS SN-table reading part to the beginning of the code, and an hdf5/parmdb implementation should be easy to create.